

## A modified model for parabolic trough solar receiver

M-C. EL JAI<sup>1</sup>, F-Z. CHALQI<sup>1</sup>

<sup>1</sup>(Lab. IMAGES. University of Perpignan. France)

**Abstract:** The aim of this paper is to give an original mathematical model that describes the heat exchange between the main components of a thermal solar collector in an Integrated Solar Combined Cycle (ISCC) plant. The obtained model is used to perform easier simulations of the studied system and gives the temperature evolutions of the heat transfer fluid and of the metal tube receiver. The model could also be used to optimize the solar collector design according to desired objectives.

**Keywords:** Distributed parameter systems, heat transfer fluid, modelling, solar parabolic trough collector.

### I. INTRODUCTION

The fight against the problem of climate change caused by pollution of air and water is increasing. It becomes overwhelmingly urgent. This is mainly due to the continued exploitation of fossil fuels resources. It is therefore essential to find a solution allowing production of CO<sub>2</sub>-free energy to meet our daily and industrial needs. The solar energy is one of the renewable energies. It is free and especially clean, and can perfectly help to solve this problem. The exploitation of this energy would be useful and more advantageous in solar plants by concentrating the sunlight. This energy can be stored as heat energy for 12 hours by using as heat transfer fluid the molten salt, the stone or the phase change materials.

The process of concentrating solar energy can be achieved by a system based on concentration of lenses, or reflective mirrors such that the sunrays converge onto a target of a smaller size and located at the focal plan of this surface.

Generally, there are two main methods used to perform the concentration of solar energy (see Fig. 1):

- Line-focusing systems: linear concentration.
- Point-focusing systems: concentration point.

In the first class, there are two types of solar plant: solar power tower (Big Solar Furnace in Odeillo, France, 1MW), and solar power of parabolic Dish-Stirling (Dish Stirling prototype plants of 10 kW each in Almeria, Spain).

In the second class, we find two types of solar plant: solar plant of parabolic trough (Nevada Solar One Power Plant, 64MW and Ain Beni-Mathar solar plant northeast Morocco, 472 MW), and solar plant of Fresnel linear collectors (PE1 solar plant in Murcia, Spain, 1.4 MW).



Fig. 1: Different methods for solar concentration

The thermodynamic solar power plants (known concentration in Fig. 2) use a lot of mirrors that make direct the solar rays to a heat transfer fluid to be heated at high temperatures. For this reason, the reflecting mirrors have to follow the sun's movement to collect and concentrate a maximum rate of solar radiation throughout the solar cycle used. The heat produced by the heat transfer fluid will be used to generate electricity using steam turbines or gas.

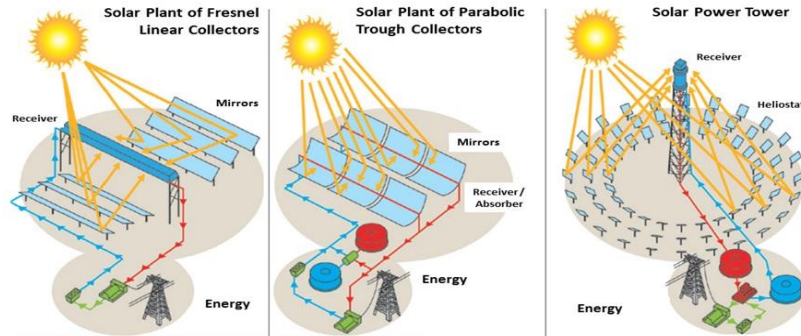


Fig. 2: Different types of solar concentration plants [1]

The technology of thermodynamic solar has current applications as power generation, solar power booster, and generation of steam for industrial processes.

In this paper, we are interested in solar plant of parabolic trough and specifically in solar plant which operating with the Integrated Solar Combined Cycle (ISCC). Here we concentrate on the case of cylindro-parabolic plants as that developed in Ain Beni-Mathar, located northeast of Morocco. The studied plant uses an integrated solar system combined with a system running a natural gas to produce electricity continuously even in the absence of the sun.

This solar plant consists of a solar field, a solar heat exchanger, two gas turbines, a steam turbine and an air condenser. The solar plant principle can be described as follows (Fig. 3). The extracted gases from the turbines are injected in two boilers. The solar energy collected by the trough parabolic mirrors, allows increasing the flow of vapor produced in the recovery boilers. An amount of water from the condenser enters the boiler. When it has been heated to the evaporation point, a part of the water will be led to the solar heat exchanger where it will be heated to the boiling point, evaporated and overheated to return then to the steam generator. It will be re-overheated before being introducing into the steam turbine of three levels (high, medium and low pressure) [2].

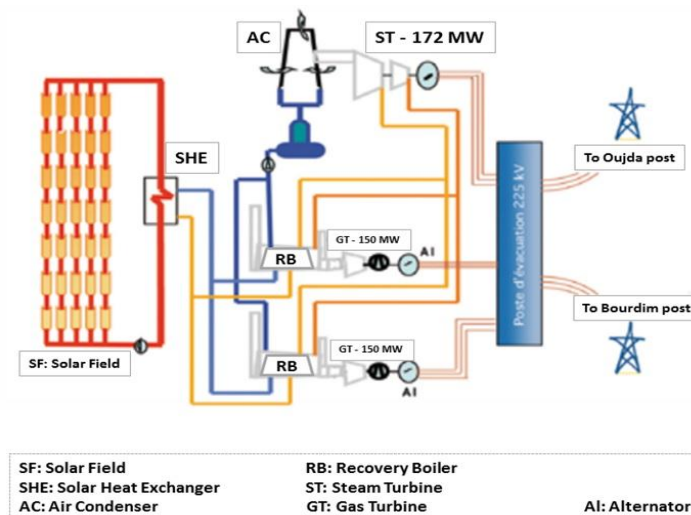


Fig. 3: Principle of Ain Beni-Mathar solar thermal plant [2].

However, the annual efficiency of these solar plants is affected by the instantaneous variations of the weather. The movement of the sun, the clouds, and the wind speed defines these variations. They are observed essentially at the parabolic trough of solar field. Therefore it is necessary to model the operating of these solar collectors for improving the efficiency of the solar field and to contribute to a better performance of the entire solar plant.

The paper is organized as follows. The next section describes the physical interactions of the solar plant components. Based on the energy balance, a general model is established. The various parameters depend strongly on the temperature of the main elements of the collector. However this model which looks simple is very complex for numerical implementation. The next section is devoted to a different writing of the model which leads to a look-like logistic model. The new version can be easily implemented and used for design or control problems. It is illustrated by simulation results.

## II. THE PHYSICAL SYSTEM

### 2.1 DESCRIPTION OF THE SOLAR FIELD

The solar plant is an Integrated Combined Cycle Thermo-Solar Power plant, located in northeast of Morocco. It consists of 256 parabolic trough solar collectors. These collectors are classified in 64 parallel loops; each loop is 618 meters long, see Fig. 4. The receiver tubes are located at the focal axis of the parabolic trough solar collectors. They contain a heat transfer fluid which temperature can reach 393 °C.

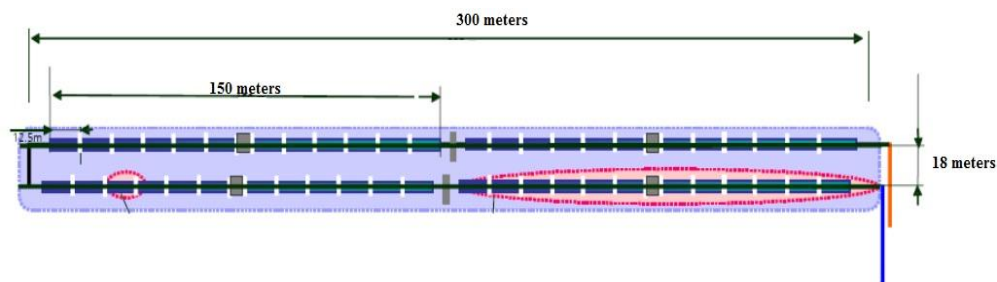


Fig. 4: The receiver loop [2]

The collector used in this solar thermal plant consists of parabolic reflectors (a series of mirrors), a metallic structure, a solar tracking system, and receiver tube. This type of parabolic trough solar collectors may have a concentration ratio of about 80%.

The mirror is made of borosilicate glass, whose transmittance is approximately 98%. This glass is covered with a layer of silver in its lower part, with a special coating and protection. The best reflector can reflect 97% of incident radiation.

The role of the solar tracking mechanism is adapted to maintain the incident solar radiation perpendicular to the reflector. The radiation is reflected to the focal line of the parabola where a receiver tube contains the heat transfer fluid.

The tube receiver or heat collection element (HCE) is of Schott PTR 70 type [3]. It is composed of two concentric tubes. The stainless-steel absorber tube, surrounded by a partially evacuated glass envelope to minimize heat losses, see Fig. 5. The receiver tube contains a heat transfer fluid which is a synthetic oil (Therminol VP-1, [4]).



Fig. 5: The solar receiver tube [3]

### 2.2 FIRST MODELLING APPROACH

Modelling parabolic trough solar collectors has been explored by many authors [5, 6, 7, 8, 9, 10]. The modelling principle is based on energy balance between the essential elements of the heat collection element (HCE) which are the receiver tube, and the heat transfer fluid. The Fig. 6 shows a transversal section of the different thermal exchanges [5, 6, 8] between the receiver tube, and the heat transfer fluid, and their environment.

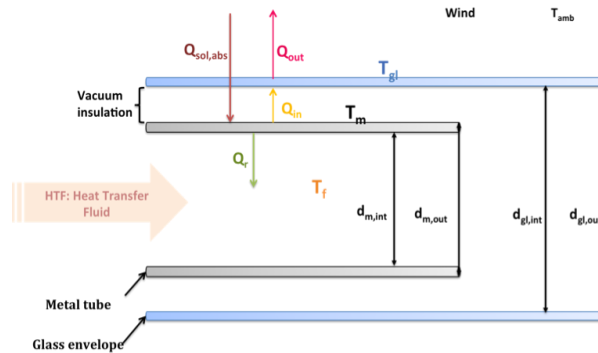


Fig. 6: Scheme of the different thermal exchanges of the HCE

The main purpose of this modelling is to predict the equilibrium temperature of the fluid at the output of the solar field generated by the flow rate at the entrance of the receiver tube. The following hypotheses are considered:

1. The properties of the fluid depend on the temperature.
2. In each section of the tube, the fluid flow is assumed to be uniformly distributed and equal to a mean
3. The solar radiation and the fluid flow vary on time and are the same for the whole receiver tube
4. The fluid is assumed to be incompressible.

The state variables we consider are the temperature of the fluid  $T_f$ , the absorber tube  $T_m$  and the glass envelope  $T_{gl}$ . The energy balance for the heat collection element leads to three partial differential equations of three temperatures. The first equation describes the fluid temperature  $T_f$ . It depends of time  $t$  and on space  $x$ . The second and third equations describe the absorber tube temperature  $T_m$  and the glass envelope temperature  $T_{gl}$ .

The obtained system of equations is then given by:

$$\left\{ \begin{aligned} \rho_f C_f A_f \frac{\partial T_f(x,t)}{\partial t} + \rho_f C_f \frac{\dot{V}_f}{N_{col}} \frac{\partial T_f(x,t)}{\partial x} &= Q_r(x,t) \\ \rho_m C_m A_m \frac{\partial T_m(x,t)}{\partial t} &= Q_{sol,abs}(x,t) - Q_{in}(x,t) - Q_r(x,t) \\ \rho_{gl} C_{gl} A_{gl} \frac{\partial T_{gl}(x,t)}{\partial t} &= Q_{in}(x,t) - Q_{out}(x,t) \end{aligned} \right. \quad (1)$$

In this system of equations, the amounts of energy were considered and defined from thermodynamics. These energies are often heat exchange between the different components of the HCE, either by convection or conduction, or radiation, taking into account the impact of the environment [5, 6, 7, 8, 10]. The heat transfer fluid, flowing inside the metal tube, receives by convection an amount of heat that depends mainly to the characteristics of fluid such as the density, the specific heat, the kinematic viscosity, the thermal conductivity [2] etc. These characteristics are related to the fluid temperature. The heat received is given by:

$$Q_r = h_{m,f} A_{surf,m,in} (T_m - T_f) \quad (2)$$

The amount of the absorbed solar energy,  $Q_{sol,abs}$ , by the parabolic trough solar collector depends on the weather and the cleanliness of the collectors and is defined by:

$$Q_{sol,abs} = I_s F(\cos\theta) D_{eff} \eta_{opt} \gamma \quad (3)$$

The two concentric tubes (metal and glass) of the receiver tube, are exchanging the heat by conduction and by radiation [5, 6, 7, 8]. This heat energy depends on the different characteristics of the stainless steel and the glass, and is defined by:

$$Q_{in} = Q_{in,rad} + Q_{in,cond} \quad (4)$$

where

$$Q_{in,rad} = \frac{\sigma A_{surf,m,out} (T_m^4 - T_{gl}^4)}{\frac{1}{\epsilon_m} + \frac{1 - \epsilon_{gl}}{\epsilon_{gl}} \frac{d_{m,out}}{d_{gl,in}}} \tag{5}$$

$$Q_{in,cond} = \frac{2 \pi k_{eff,air} (T_m - T_{gl})}{\ln(\frac{d_{gl,in}}{d_{m,out}})} \tag{6}$$

An amount of thermal energy is exchanged, by convection and radiation [5, 6, 7, 8], between the glass envelope and the environment. This thermal energy is defined by the characteristics of the glass and those defining the ambient air, as follows:

$$Q_{out} = Q_{out,rad} + Q_{out,conv} \tag{7}$$

where

$$Q_{out,rad} = \sigma \epsilon_{gl} A_{surf,gl,out} (T_{gl}^4 - T_{amb}^4) \tag{8}$$

$$Q_{out,conv} = h_{gl,amb} A_{surf,gl,out} (T_{gl} - T_{amb}) \tag{9}$$

After replacing in equations (1) and dividing by  $\rho CA$  for each, we obtain a system of partial differential equations (PDE) which can be rewritten in the following simple form

$$\left\{ \begin{aligned} \frac{\partial T_f(x,t)}{\partial t} + \alpha_0 \frac{\partial T_f(x,t)}{\partial x} &= a_1 T_f + a_2 T_m \\ \frac{\partial T_m(x,t)}{\partial t} &= b_1 T_f + b_2 T_m + b_3 T_{gl} + b_4 T_m^4 + b_5 T_{gl}^4 + b_6 \\ \frac{\partial T_{gl}(x,t)}{\partial t} &= c_1 T_m + c_2 T_{gl} + c_3 T_m^4 + c_4 T_{gl}^4 + c_5 \end{aligned} \right. \tag{10}$$

where the coefficients  $a_i$ ,  $b_i$  and  $c_i$  are given in the annex. The model of the solar trough collector allows the knowledge of the fluid temperature evolution only at the output of the receiver tube. Furthermore it could help to choose the parameters of the plant in such a way that the temperature can be maintained at a desired equilibrium value, despite instantaneous variations of the weather. This could be regulated by a convenient flow rate at the entrance of the receiver tube. However numerical simulation of the complete obtained model above (10), leads to various difficulties, due to the complexity of the model coefficients which all depend nonlinearly on the temperature.

So it becomes necessary to modify the obtained model for easier simulations. The first assumption is to assume that a perfect vacuum exists between the two concentric metal and glass tubes. In this case we can neglect the glass behavior and thus we obtain a system coupling fluid and metal temperatures dynamics. This assumption allows to study the heat exchange between the fluid and the metal tube. The first exchange describes the amount  $Q_g$  of energy defined in equation (2), while the second exchange is defined by  $Q_{abs,sol} - Q_g - Q_{m,amb}$ . The amount of energy  $Q_{m,amb}$  describes the heat exchange between the metal tube and its environment. This thermal energy is given by :

$$Q_{m,amb} = h_{m,amb} A_{surf,m,out} (T_m - T_{amb})$$

Finally the model can be described by a model reformulated as follows

$$\left\{ \begin{aligned} \rho_f C_f A_f \frac{\partial T_f(x,t)}{\partial t} + \rho_f C_f \frac{\dot{V}_f}{N_{col}} \frac{\partial T_f(x,t)}{\partial x} &= h_{m,f} A_{surf,m,in} (T_m - T_f) \\ \rho_m C_m A_m \frac{\partial T_m(x,t)}{\partial t} &= I_z F(\cos\theta) D_{eff} \eta_{opt} \gamma - h_{m,amb} A_{surf,m,out} (T_m - T_{amb}) \\ &\quad - h_{m,f} A_{surf,m,in} (T_m - T_f) \end{aligned} \right. \tag{11}$$

which can be simplified to the following form

$$\begin{cases} \frac{\partial T_f(x,t)}{\partial t} + a_0 \frac{\partial T_f(x,t)}{\partial x} = a_1 T_f + a_2 T_m \\ \frac{\partial T_m(x,t)}{\partial t} = b_1 T_f + \beta_1 T_m + \beta_2 \end{cases} \quad (12)$$

Where, the coefficients  $\beta_i$  are different from the  $b_i$ 's and are given in the annex. One can notice that the various coefficients depend on the temperature of the fluid or the metal tube

### III. MODIFIED MODEL

Firstly the model (12) can be easily studied from mathematical point of view. For that purpose we rewrite it in a matrix form, by considering the vector  $z$  defined by  $z = \begin{pmatrix} T_f \\ T_m \end{pmatrix}$ . Thus the above system can be easily represented in the following vector form

$$\dot{z} = A_1 z + B_1 \quad (13)$$

Where  $A_1$  is a matrix of order  $(2 * 2)$  and  $B_1$  is a matrix of order  $(2 * 1)$ , defined by

$$A_1 = \begin{pmatrix} -a_0 \frac{\partial}{\partial x} + a_1 & a_2 \\ b_1 & \beta_1 \end{pmatrix} \text{ and } B_1 = \begin{pmatrix} 0 \\ \beta_2 \end{pmatrix} \quad (14)$$

This formulation shows that the considered system is well posed from mathematical point of view and, under the condition that the coefficients are bounded, the system admits a unique solution. In what follows we consider the model (12) and we explore some coefficients which affect dramatically the resolution. In spite of the simplicity of the model (12), it is not consistent with the nature of the system. Furthermore its numerical implementation leads to surprising numerical results. It is difficult to find in the literature models which can lead to realistic simulations. Most of the models describe very complex physics but lead to non possible simulations. A model can be considered as a fine model if it is simple and can be implemented easily for simulations. That is why we consider a modified model which could be used by solar plant modelers without complex physical considerations.

#### 3.1 MODELLING APPROACH

The main difficulties in the above model are due to the temperatures sensitivity with respect to the model coefficients. However we have noticed that some of the coefficients depend nonlinearly of the temperature. Various simulations show that the solution evolves dramatically for small variations of certain coefficients. A numerical study of the coefficients leads to a second assumption which consists to neglect the coefficients which value are lower than  $10^{-10}$ . On an other hand the coefficients  $\alpha_1$  and  $\beta_1$  are slightly linear with respect to the fluid temperature  $T_f$  as shown in Fig. 7.

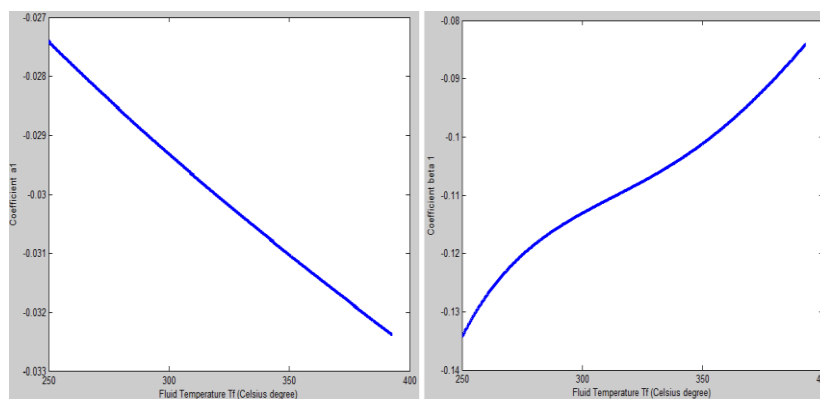


Fig. 7: Evolution of the coefficients  $\alpha_1$  and  $\beta_1$

This suggests to consider a linear description for these coefficients and to reformulate the system under the form

$$\left\{ \begin{aligned} \frac{\partial T_f(x,t)}{\partial t} + a_0 \frac{\partial T_f(x,t)}{\partial x} &= (\alpha_{a_1} T_f + \beta_{a_1}) T_f + a_2 T_m \\ \frac{\partial T_m(x,t)}{\partial t} &= b_1 T_f + (\alpha_{\beta_1} T_f + \beta_{\beta_1}) T_m + \beta_2 \end{aligned} \right. \quad (15)$$

In the first equation of (15) the term  $(\alpha_{a_1} T_f + \beta_{a_1})$  can be rewritten in the form

$$\alpha_{a_1} T_f + \beta_{a_1} = -\alpha_{a_1} [K - T_f]$$

where  $\beta_{a_1} = \alpha_{a_1} K$ . Thus the first equation can be stated by

$$\frac{\partial T_f(x,t)}{\partial t} + a_0 \frac{\partial T_f(x,t)}{\partial x} = -\alpha_{a_1} [K - T_f] T_f + a_2 T_m \quad (16)$$

This formulation can be seen as equations of an equilibrium model where the temperature will be stabilized around a certain value. One can consider other approaches for the coefficients modelization but they do not lead to any improvement of the model.

### 3.2 SIMULATIONS

The obtained model consists in a system of two nonlinear partial differential equations.

$$\left\{ \begin{aligned} \frac{\partial T_f(x,t)}{\partial t} + a_0 \frac{\partial T_f(x,t)}{\partial x} &= -\alpha_{a_1} [K - T_f] T_f + a_2 T_m \\ \frac{\partial T_m(x,t)}{\partial t} &= b_1 T_f + \alpha_{\beta_1} T_f T_m + \beta_{\beta_1} T_m + \beta_2 \end{aligned} \right. \quad (17)$$

It evolves in time  $t$  and depends on one-dimensional space  $x$ . Formally it derives from the system (12) and therefore it is well posed from mathematical point of view.

In this section we give a numerical approach for the resolution of (17). The discretization principle for solving boundary-value problems consist of replacing each of the derivatives in the differential equation by an approximate difference quotient approximation. The difference quotient is generally chosen so that a certain approximation order error is maintained. Other methods for solving (finite elements) these equations could be considered.

The model (17) is explicitly nonlinear. In this system, we know the mean values for all the remaining coefficients. The range of variation of the temperature can lead to an explicit approximation of the coefficients. Thus we find the following mean values for the considered coefficients:

$\alpha_{a_1} = -3.46610^{-5}$	$\beta_{a_1} = -0.0188$
$\alpha_{\beta_1} = 3.2210^{-4}$	$\beta_{\beta_1} = -0.2141$

For the discretization let  $L$  be the length of a loop of the HCE and  $\Delta x$  a step size. Denote  $N_x$  the number of space paths of length  $\Delta x$  (see Fig. 8), then  $\Delta x = L/N_x$ . In the considered plant we have  $L = 61.8$  meters. For the time horizon, we consider the time step denoted  $\Delta t$  and  $N_t$  the number of time steps. If we denote  $t_{\text{period}}$  the time length between the sunrise and the sunset (with a maximum solar flux), then  $\Delta t = t_{\text{period}}/N_t$ .

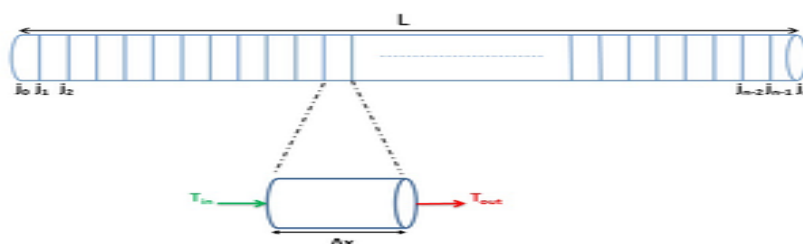


Fig. 8: Discretization of the heat collection element

The resolution of the reformulated model requires initial and boundary conditions. We assume that  $T_f(0, x) = T_{f,0}$  the initial known temperature of the fluid. We also denote  $T_{in}(0, x) = T_{in,0}$ , the initial temperature of the metal tube, assumed to be known. In practical applications we consider  $T_{in,0} = T_{f,0}$ .

3.2.1 TIME EVOLUTION TEMPERATURES

The model previously modified is given in (17) where  $T_f$  is the fluid temperature and  $T_{in}$  is the metal tube temperature. For the time evolution of the fluid temperature at any point of the receiver tube, it is not necessary to consider the space evolution. So we consider firstly that the partial derivative in space vanishes, thus the first equation of (17) becomes

$$\frac{\partial T_f(x, t)}{\partial t} = -\alpha_{a1} [K - T_f] T_f + \alpha_2 T_m \tag{18}$$

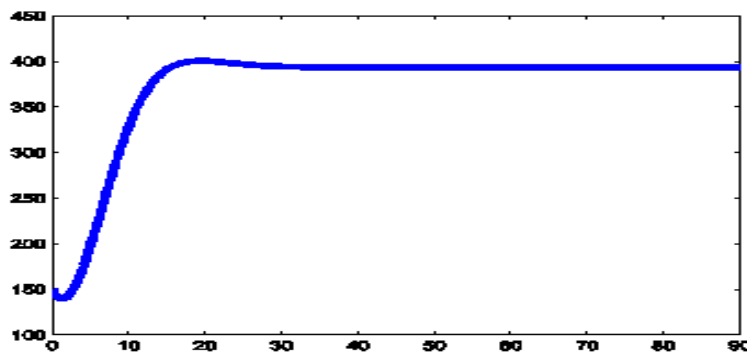


Fig. 9: Evolution of the fluid temperature  $T_f$ .

In this case we neglect the space variable and denote

$$T_f^n \cong T_f(n\Delta t)$$

and we apply a modified Euler method (more accurate) with the initial conditions  $T_{f,0}$  and  $T_{in,0}$ . Then we obtain the evolution graphs given in Fig. 9 for the fluid temperature and in Fig. 10 for the metal tube temperature.

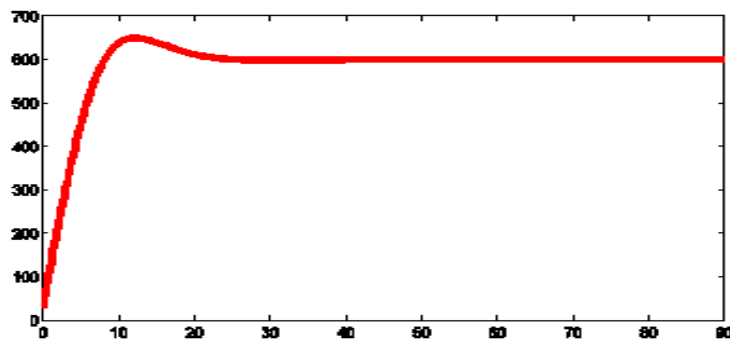


Fig. 10: Time evolution of the metal tube temperature  $T_{in}$ .

We notice that the metal tube temperature is always higher than that of the fluid. For the fluid and the receiver tube the figures show that the temperature evolves until an equilibrium level which maintains the fluid temperature at about 400° Celsius. These results are consistent with the measurements obtained by the output, under ideal conditions.

Remark 3.1

In the applications depending on the considered plant one can introduce a weighting term  $\xi$  to adapt the evolution of the fluid temperature (which may depend on physical parameters and day insulation). For that purpose we can rewrite the term  $\alpha_{a1} T_f + \beta_{a1} [K - T_f]$  considering

$$\alpha_{a_1} T_f + \beta_{a_1} = -\alpha_{a_1} [K - \xi T_f]$$

The figure (11) shows the influence of the coefficient  $\xi$  on the time evolution of the fluid temperature.

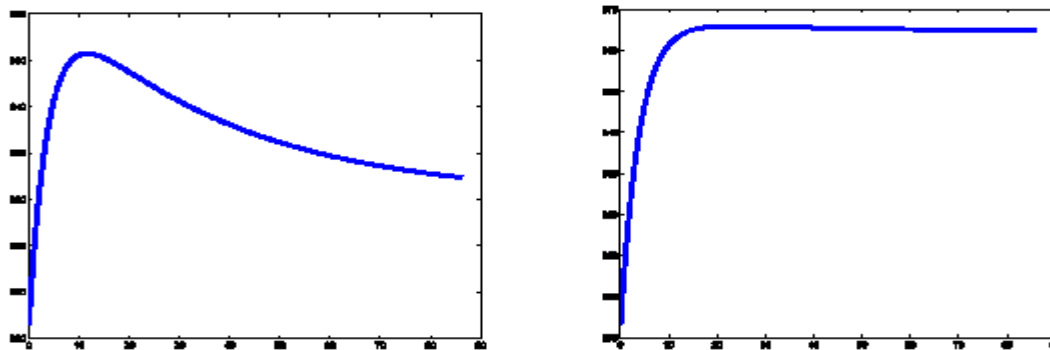


Fig. 11: Evolution of the fluid temperature  $T_f$  in time in the cases where the weighting term  $\xi = 0.19$ , and  $\xi = 0.16$

The Fig. 11 shows that at the beginning of the time interval, and for a weighting term equal to 0.19, the fluid temperature  $T_f$  increases with time to a maximum value ranging from 352°C to 362°C. Then the fluid temperature  $T_f$  decreases to a value of about 324°C. However when the weighting term  $\xi$  is equal to 0.16, the fluid temperature  $T_f$  increases with time to reach a maximum value of about 365.9°C and remains maintained at this value. The weighting term  $\xi$  can be used in the discretized equation for an adaptation of the evolution to any situation.

3.2.2 TIME AND SPACE EVOLUTION OF THE TEMPERATURES

Introduce now the mesh points of coordinates  $\{j\Delta x, n\Delta t\}$ , for  $n = 1, 2, \dots, N_t$  and  $j = 1, 2, \dots, N_x$  and let  $T_i^n$  be an approximated value of the temperature  $T(j\Delta x, n\Delta t)$  ( $T_f$  for the fluid and  $T_m$  for the metal tube) denoted

$$T_j^n \cong T(j\Delta x, n\Delta t)$$

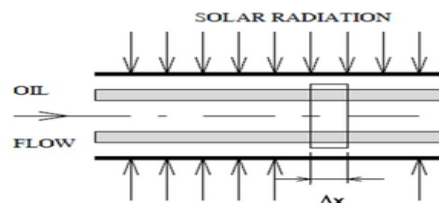


Fig. 12: Element of the distributed parameter model

With these notations we illustrate the efficiency of the given model considering the following finite difference first order approximations of the derivatives

$$\frac{\partial T(j\Delta x, n\Delta t)}{\partial t} = (T_j^{n+1} - T_j^n) / \Delta t \quad \text{and} \quad \frac{\partial T(j\Delta x, n\Delta t)}{\partial x} = (T_j^n - T_{j-1}^n) / \Delta x \quad (19)$$

The resolution of the reformulated model requires initial and boundary conditions. The initial conditions have been stated in previous section. Additionally we consider boundary condition at the entrance of the receiver tube given by  $T_f(t, 0) = T_{f_0}$  and  $T_m(\tau, 0) = T_{m_0}$  assumed to be known.

In this case, we have to discretize the principal model in equation (17). Denote  $\tau = \Delta t, \Delta x$  and apply the finite difference discretization in time and space given in (19) (see [11]), we obtain

$$\begin{cases} T_{f,j}^{n+1} = [1 - ra_0 - \Delta t \alpha_{a_1} (K - T_{f,j}^n)] T_{f,j}^n + ra_0 T_{f,j-1}^n + \Delta t a_2 T_{m,j}^n \\ T_{m,j}^{n+1} = \Delta t \alpha_{\beta_1} T_{f,j}^n T_{m,j}^n + \Delta t b_1 T_{f,j}^n + [1 + \Delta t \beta_{\beta_1}] T_{m,j}^n + \Delta t \beta_2 \end{cases} \quad (20)$$

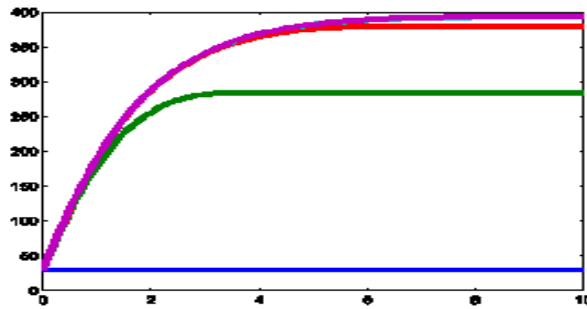


Fig. 13: Global (time-space) temperature evolution of the fluid

For the illustrative simulation, we have considered a time step equal to 0.005 second and a space step equal to 0.1 meter.

The Fig. 13 presents the obtained results for the fluid temperature  $T_f$  throughout the receiver tube at different times, and Fig. 14 that of the metal tube  $T_{ill}$ .

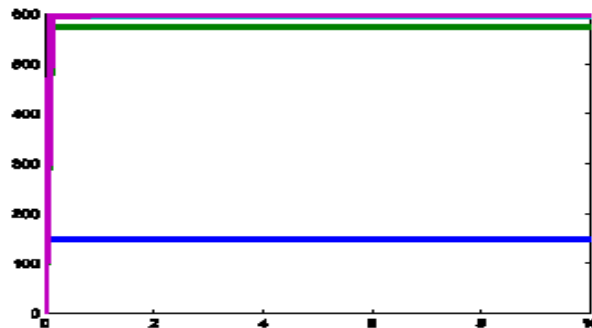


Fig. 14: Global (time-space) temperature evolution of the metal tube.

The Fig. 13 and 14 show that the temperatures increase from initial temperature at the entrance of the tube to reach a maximal value of about 400°C for the fluid and 600°C for the metal tube. The metal tube temperature reaches its equilibrium value very quickly all along the tube, because all the tube is in the focal line of the solar receiver and is directly exposed to the sunlight.

The nomenclature and the annex after would help to achieve the illustrative simulations.

**Remark 3.2**

The modified model introduced in the previous section has reduced the model to a system of two differential equations (17). We can notice that the receiver tube is all located in the focal line of the parabolic trough. Consequently we can consider that the whole receiver tube is excited by the same amount of energy and thus its temperature is equal to a mean value  $T^*$ .

This is obviously illustrated by the Fig. 14. Additionally the users could be interested only by the fluid temperature evolution and not that of the metal tube. This suggests that the fluid receives the same amount of energy all along the tube which can be considered as a passive control on the fluid. Therefore we can simplify the model by neglecting the receiver tube equation and considering that the fluid is excited by its contact with the metal tube, by a certain amount to be identified. This allows to consider the following simplified partial differential equation which state is the fluid temperature  $T_f$

$$\frac{\partial T_f(x,t)}{\partial t} + a_0 \frac{\partial T_f(x,t)}{\partial x} = -\alpha_{a_1} [K - T_f] T_f + a_2 \tilde{T} \tag{21}$$

where  $T^*$  is assumed to be known. The system is augmented by initial and boundary conditions.

We can assume that the mean value  $T^*$  is equal to that given by measurements of the metal tube temperature. In this case the various coefficients of the model do not fit with the physical values of the previous model. Thus the model can be improved using an identification of the other coefficients  $\alpha_{a_1}, \alpha_{a_2}, \alpha_{a_3}, \alpha_{a_4}$ . The following figures show that the results are very significant and that the model can be drastically reduced.

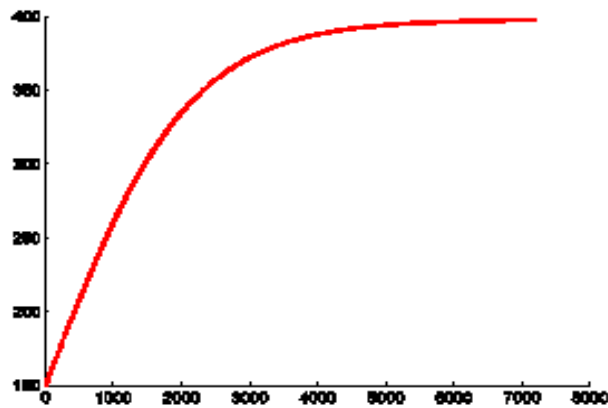


Fig. 15: Fluid temperature evolution (at a fixed point of the tube) without considering the space impact.

The numerical simulations have been achieved considering the following values:  $\alpha_0 = 0.04$ ,  $\alpha_1 = 2 \cdot 10^{-6}$ ,  $K = 310$  and  $\alpha_2 = 0.07$ .

The Fig. 15 shows that the result is quite similar to that of the complex model considered in the first section.

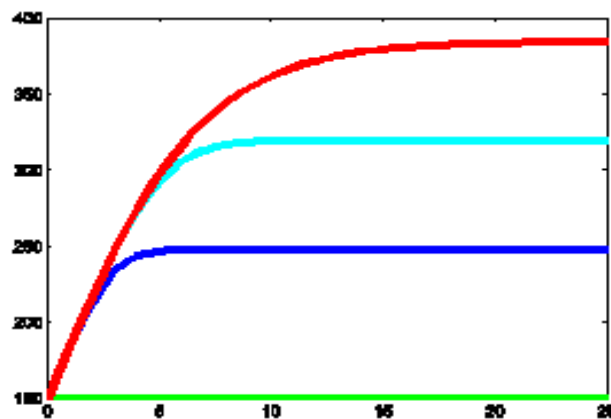


Fig. 16: Fluid temperature evolution, at different times, all along the receiver tube

The Fig. 15 and 16 show that the temperature level at the end of the tube is about 375°. This temperature level can be adjusted and regulated at any convenient desired level, depending of the real conditions of the trough solar receiver.

#### IV. CONCLUSION

In this paper we give an original modified model of the heat collector element within an Integrated Combined Cycle Thermo-Solar Power Plant. The given approach is more accurate and easier to implement. This model has necessitated the study of heat exchange between the three components of the heat collection element. The reformulation of the model was based by considering a perfect vacuum between the two concentric tubes (metal tube inside the glass envelope) of the heat collection element (HCE). The model established consists in two first order partial differential equations depending on time and one dimension space variable, and may be reduced to one partial differential equation. The different simulation results show that both the fluid temperature  $T_f$  and the metal tube temperature  $T_m$  evolve until reaching a certain equilibrium value. The obtained results are consistent with the plant values. The proposed model can be improved by considering an identification of some of the coefficients. This identification depends on the considered solar plant and will be explored in a future work.

#### V. ACKNOWLEDGEMENTS

We would like to thank

- 1) Professor A. EL JAI (University of Perpignan, France) for his advice throughout this work; as well for modelling aspects as for numerical approach of the studied problem.
- 2) Lorenzo Castro Gómez-Valadés, Process Engineer (ISCC Ain Beni Mathar Morocco), for his kind help and the data of the ISCC plant.

## REFERENCES

- [1]. S. Andrieux, Le solaire thermodynamique à concentration, 2012, 1-4.
- [2]. F-Z. CHALQI, Bilan thermique de la central thermo-solaire d'Ain Béni-Mathar (ABM), Université de Perpignan Via Domitia, Août 2012.
- [3]. Schott Solar Csp Gmbh, Schott PTR 70 Receivers, Mainz (Germany), 2009.
- [4]. Solutia, Therminol VP-1, Louvain-la-Neuve (France), 2002.
- [5]. Thorsten A. Stuetzle, Automatic Control of the 30 MWe SEGS VI Parabolic Trough Plant, University of Wisconsin-Madison, Madison, 2002.
- [6]. R. Forristall, Heat transfer analysis and modeling of a parabolic trough solar receiver implemented in engineering equation solver, Technical report, National Renewable Energy laboratory, 2003.
- [7]. N. Hamani, A. Moumami, N. Moumami, A. Saadi and Z. Mokhtari, Simulation de la température de sortie de l'eau dans un capteur solaire cylindro-parabolique dans le site de Biskra, Revue des Energies renouvelables, Vol. 10. N°2, 2007, 215-224.
- [8]. F. Burkholder and C. Kulscher, Heat loss testing of Schott's 2008 PTR70 parabolic trough receiver, Technical report (NREL/TP-550-45633. May 2009).
- [9]. B. Kelly and D. Kearney, Parabolic Trough Solar System Piping Model, Final Report, National Renewable Energy laboratory, 2006.
- [10]. Ming Qu, D. H. Archer and S. V. Masson, A linear Parabolic trough Solar Collector Performance Model, Renewable Energy Resources and a Greener Future Vol.VIII-3-3, Proceedings of the Sixth International Conference for Enhanced Building Operations, Shenzhen, China, November 6 - 9, 2006.
- [11]. A. El Jai, Eléments d'analyse numérique (PUP, 2nd edition, 2010).

## ANNEX

$\rho_f$  : HTF density

$\rho_{m}$  : Metal (Stainless steel) density

$\rho_{gl}$  : Glass density

$C_f$  : HTF specific heat

$C_m$  : Metal (Stainless steel) specific heat

$C_{gl}$  : Glass specific heat

$d_{m, in}$  : Inside diameter of the metal tube

$d_{m, out}$  : Outside diameter of the metal tube

$d_{gl, in}$  : Inside diameter of the glass

$d_{gl, out}$  : Outside diameter of the glass

$A_f$  : Noted also  $A_{m, in}$ . Cross-sectional area inside the metal tube

$A_m$  : Cross-sectional area of the metal tube

$A_{gl}$  : Cross-sectional area of the glass

$A_{solar, m, in}$  : Inner surface area per length of the metal tube

$A_{solar, m, out}$  : Outer surface area per length of the metal tube

$A_{solar, gl, out}$  : Outer surface area per length of the glass envelope

$I_s$  : Solar Direct irradiance

$F(\cos \theta)$  : Incidence modifier function

$\theta$  : Angle of incidence, degree

$D_{eff}$  : Effective width of the collector

$\eta_{dirt}$  : Optical efficiency: Factor depending of dirt on the mirrors

$k_{eff, air}$  : Effective thermal air conductivity

$T_{amb}$  : Ambient temperature

$\dot{V}_f$  : Overall HTF volume flow rate

$N_{col}$  : Total number of collectors

$\epsilon_m$  : Metal (Stainless steel) emissivity

$\epsilon_{gl}$  : Glass emissivity

$\sigma$  : Stefan-Boltzmann constant

$h_{m, f}$  : Convection heat transfer coefficient between the metal tube and the HTF

$h_{gl, amb}$  : Convection heat transfer coefficient between the glass and the ambient

$h_{m, amb}$  : Convection heat transfer coefficient between the metal tube and the ambient.